JSHC
Japan Society of Histochemistry and Cytochemistry
Established 1959

Acta Histochem. Cytochem. 46 (2): 97–104, 2013
doi:10.1267/ahc.13006

Altered Dynamics in the Renal Lymphatic Circulation of Type 1 and Type 2 Diabetic Mice

Takanobu Uchiyama[1], Shunsuke Takata[1], Hiroyuki Ishikawa[1] and Yoshihiko Sawa[2]

[1]Department of Oral Growth & Development, Fukuoka Dental College 2–15–1 Tamura, Sawara-ku, Fukuoka 814–0193, Japan and
[2]Department of Morphological Biology, Fukuoka Dental College 2–15–1 Tamura, Sawara-ku, Fukuoka 814–0193, Japan

Received February 6, 2013; accepted March 26, 2013; published online April 12, 2013

The dynamics of the renal lymphatic circulation in diabetic nephropathy is not fully elucidated. The present study evaluated the effect of diabetic nephropathy on the renal lymphatic circulation in streptozotocin (STZ)-induced type 1 diabetic mice (ICR-STZ) and in type 2 diabetic KK/Ta mice which were fed a high fat diet (KK/Ta-HF). The diabetic mouse kidneys developed edema because of the nephropathy. In control mice renal lymphatic vessels distributed in the cortex but rarely in the medulla while in ICR-STZ and KK/Ta-HF mice, there were many lymphatic vessels with small lumen in both cortex and medulla. Total numbers and areas of renal blood vessels in the diabetic mice were similar to those in the controls while the total numbers and areas of renal lymphatic vessels were larger in diabetic mice than in the controls. There were statistically significant differences in the numbers of lymphatic vessels with diameters of 50–100 μm between the ICR-STZ and the control ICR mice, and in the numbers of lymphatic capillaries with diameters smaller than 50 μm between the KK/Ta-HF and the control KK/Ta mice. The diabetic nephropathy may induce the lymphangiogenesis or result in at least the renal lymphatic vessel expansion.

Key words: kidney, lymphatics, diabetes, nephropathy, lymphangiogenesis

I. Introduction

Diabetes mellitus is a common disease in Japan affecting approximately 2.7 million people. The 95% of diabetes mellitus is type 2 diabetes associated with metabolic disorders while type 1 diabetes is a failure of glucose metabolism based on insulin deficiencies arising from the autoimmune destruction of insulin-secreting β cells. Elevated glucose levels lead cardiovascular systems to induce both proinflammatory cytokine production and oxidative stress, therefore, diabetes mellitus results in microvascular complications to peripheral arteries [2, 19, 23]. Approximately 20–30% of patients with diabetic nephropathy develop renal insufficiency. Type 1 diabetic patients often have enlarged kidneys with an elevation in the glomerular filtration rate. Without specific treatment, 80% of type 1 diabetic patients with persistent microalbuminuria progress to overt nephropathy within 15 years and more than 75% of overt nephropathy sufferers shift to end-stage renal disease within 20 years. Type 2 diabetic patients often have microalbuminuria at the time of the first diabetic diagnosis and 20% of type 2 diabetes patients with overt nephropathy will progress to end-stage renal disease within 20 years based on the high mortality rate of cardiovascular disease prior to progression to end-stage renal disease. It is known that a family history of end-stage renal disease and hypertension, and defects in the angiotensin-converting enzyme and the sodium proton pump are significant risk factors for the renal failure development [2, 19, 23].

Diabetic nephropathy is a progressive glomerulosclerosis caused by excess accumulation of extracellular matrix overproduced by mesangial cells with increased formation of advanced glycation end products like Nε-carboxymethyl lysine, and with secretion of various cyto-

Correspondence to: Yoshihiko Sawa, DDS, Department of Morphological Biology, Fukuoka Dental College, 2–15–1 Tamura, Sawara-ku, Fukuoka 814–0193, Japan.
E-mail: ysawa@college.fdcnet.ac.jp

kines such as transforming growth factor-β (TGF-β) from podocytes, glomerular endothelial cells, mesangial cells, and leukocytes in the glomeruli. Characteristics of diabetic nephropathy include mesangial expansion, loss of podocytes, glomerular hyperplasia, thickening of the glomerular basement membrane, and tubular epithelial cell dysfunction. The mesangium finally causes the occlusion of the glomerular capillaries under a diabetic milieu [6, 16, 17, 22]. There are many reports of the biology of diabetic nephropathy, but little is known about the dynamics of the renal lymphatic circulation in diabetic nephropathy. Renal lymphangiogenesis occurs in chronic interstitial nephritis and kidney transplants [14]. Therefore, it is thought that nephropathy is a cause of the renal circulation developing to the pro-lymphangiogenic state as a compensatory response to renal edema and hypertension. This study aimed to investigate the effect of the diabetic nephropathy on the renal lymphatic circulation in type 1 and type 2 diabetic model mice.

II. Materials and Methods

Experimental animals

This study used KK/TaJcl (KK/Ta) mice as a mouse model with type 2 diabetes and the streptozotocin (STZ)-induced diabetic mice (ICR-STZ) as a mouse model with type 1 diabetes [15, 21]. The protocol for the animal use was reviewed and approved by the animal experiment committee of Fukuoka Dental College in accordance with the principles of the Helsinki Declaration. Five-week-old male ICR mice (n=5) (Japan Clea Inc., Osaka, Japan) were given a single intraperitoneal injection of STZ (200 mg/kg body weight) (Sigma, St. Louis) in a 0.05 M citric acid buffer at pH 4.5 (20 mg/ml). One week after the STZ injection, diabetes was confirmed by measurement of the blood glucose using a Glutest Sensor (Sanwa Kagaku Kenkyusyo CO., LTD., Nagoya, Japan), and we designated ICR-STZ mice with blood glucose above 600 mg/dl for four months as insulin-dependent type 1 diabetic mice. Nine-week-old male KK/Ta mice (n=5) (Japan Clea Inc., Osaka, Japan) with a genetic background of insulin-independent diabetes were fed a high fat diet feed for diabetes mellitus studies (HFD32, Japan Clea) for five months, and we designated KK/Ta mice with blood glucose above 600 mg/dl as type 2 diabetic mice (KK/Ta-HF). The controls were ICR mice given a 0.05 M citric acid buffer and nine-week-old male KK/Ta mice before feeding with HFD32.

Immunohistochemistry

The collection of the mouse tissue was conducted after euthanasia by induction anesthesia of the mice with 2% Isoflurane (1 l/min) and intraperitoneal injections with sodium pentobarbital (10 ml/kg, Nembutal, Abbott Laboratories, North Chicago, IL). Frozen 10 μm sections cut in a cryostat and placed on slide glasses were fixed in 100% methanol for 5 min at –20°C. The sections were treated with 0.1% goat serum for 30 min at 20°C and then the sections were treated with PBS containing 0.1% goat serum and primary antibodies (1 μg/ml): hamster monoclonal anti-mouse podoplanin (AngioBio Co., Del Mar, CA) as a marker of podocyte and lymphatic endothelium, and rabbit polyclonal anti-mouse platelet endothelial cell adhesion molecule-1 (PECAM-1, Abcam) as a marker for blood endothelium for 8 hr at 4°C. After the treatment with the primary antibodies the sections were washed three times in PBS for 10 min and immunostained for 0.5 hr at 20°C with 0.1 μg/ml of second antibodies: Alexa Fluor (AF) 488 or 568-conjugated goat anti-hamster or anti-rabbit IgGs (Probes Invitrogen Com., Eugene, OR). The immunostained sections were mounted in 50% polyvinylpyrrolidone solution.

Measurement of the number of vasculature

The immunostained mouse kidney sections were examined by fluorescence microscopy (BZ-8100, Keyence Corp., Osaka, Japan). The numbers of PECAM-1-stained blood vessels and podoplanin-stained lymphatic vessels were counted at five different areas (0.9 mm×0.7 mm). All experiments were carried out five times, repeatedly, and data are expressed as means±standard deviations (SD). Statistically significant differences ($p<0.01$) were determined by the unpaired two-tailed Student's t test with STATVIEW 4.51 software (Abacus concepts, Calabasas, CA).

Measurements of the areas of vasculature

The area of PECAM-1-stained blood vessels and podoplanin-stained lymphatic vessels were measured at ten different spots (0.36 mm×0.36 mm) in the renal section images at 100× magnification using ImageJ (National Institutes of Health, Bethesda, MD). All experiments were carried out five times, repeatedly, and data are expressed as means±SD. Statistically significant differences ($p<0.01$) were determined by the unpaired two-tailed Student's t test with STATVIEW 4.51 software (Abacus).

III. Results

Immunohistochemical examination of lymphatic vessels in the diabetic mouse kidneys

The ICR-STZ mouse kidneys were light gray and statistically significantly larger than the ICR control mice (ICR-STZ vs ICR=length 14.55±1.34 mm vs 11.75±0.27 mm; width 8.53±0.41 mm vs 7.27±0.65 mm) (Fig. 1). In the immunostaining for podoplanin and PECAM-1 in the mouse heart sections, narrow lymphatic vessels were immunostained by anti-podoplanin and blood vessels with opened lumen were immunostained by anti-PECAM-1 but not by anti-podoplanin (Fig. 1B). None of the negative controls had no cross reactions with primary and secondary antibodies, and there were no differences in the fluorescence intensity of the target protein of the simple immunostaining with anti-PECAM-1 or anti-podoplanin and the

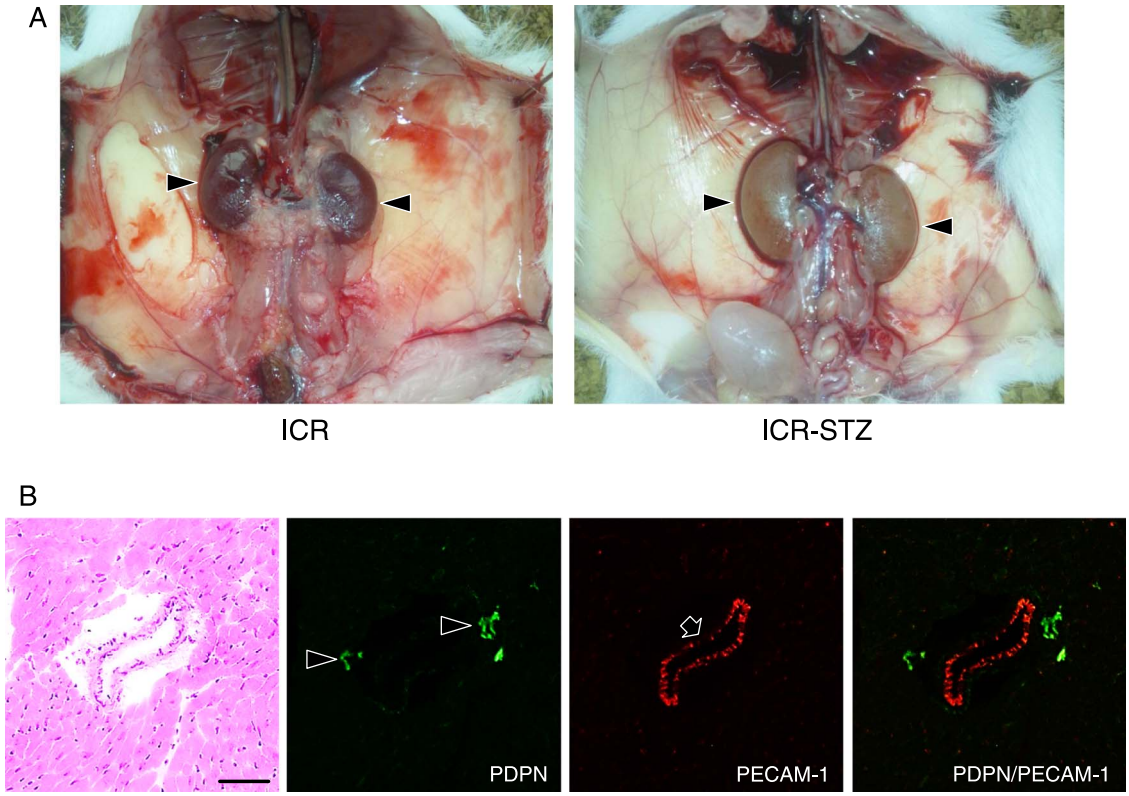

Fig. 1. (**A**) Macroscopic views of ICR and ICR-STZ mouse kidneys. The kidneys of the ICR control mouse show blood color while the ICR-STZ mouse kidneys with diabetic nephropathy show light gray. The size of the kidneys is significantly larger in the ICR-STZ mice than in the ICR mice. (**B**) Immunostaining for podoplanin and PECAM-1 in the mouse tongue sections. Narrow lymphatic vessels (arrowheads) are immunostained by anti-podoplanin. Blood vessels with opened lumen (arrows) are immunostained by anti-PECAM-1 but not by anti-podoplanin. Bar=100 μm.

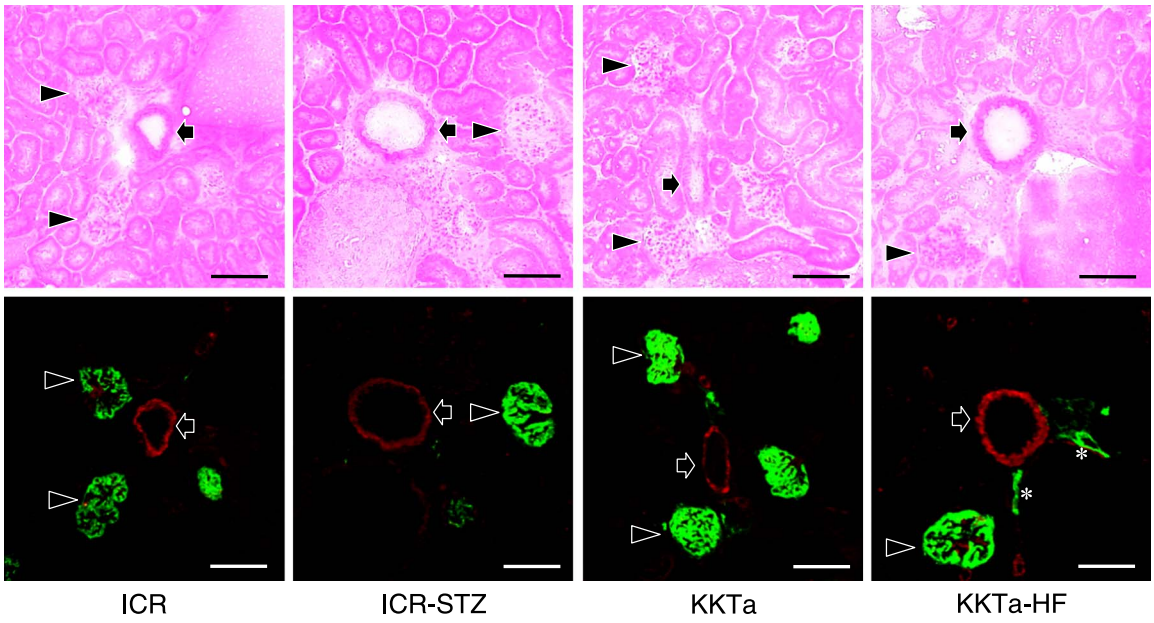

Fig. 2. Immunostaining for podoplanin and PECAM-1 in the diabetic mouse kidney cortex. The immunostained sections were re-stained by HE staining. In the ICR, ICR-STZ, KKTa, and KK/Ta-HF mice, anti-podoplanin reacted to glomeruli (arrowheads) and to lymphatic vessels with narrow lumens (asterisks), but not to blood vessels with rounded lumens (arrows). Anti-PECAM-1 reacted to blood vessels and weakly to glomerular capillaries. Bar=100 μm.

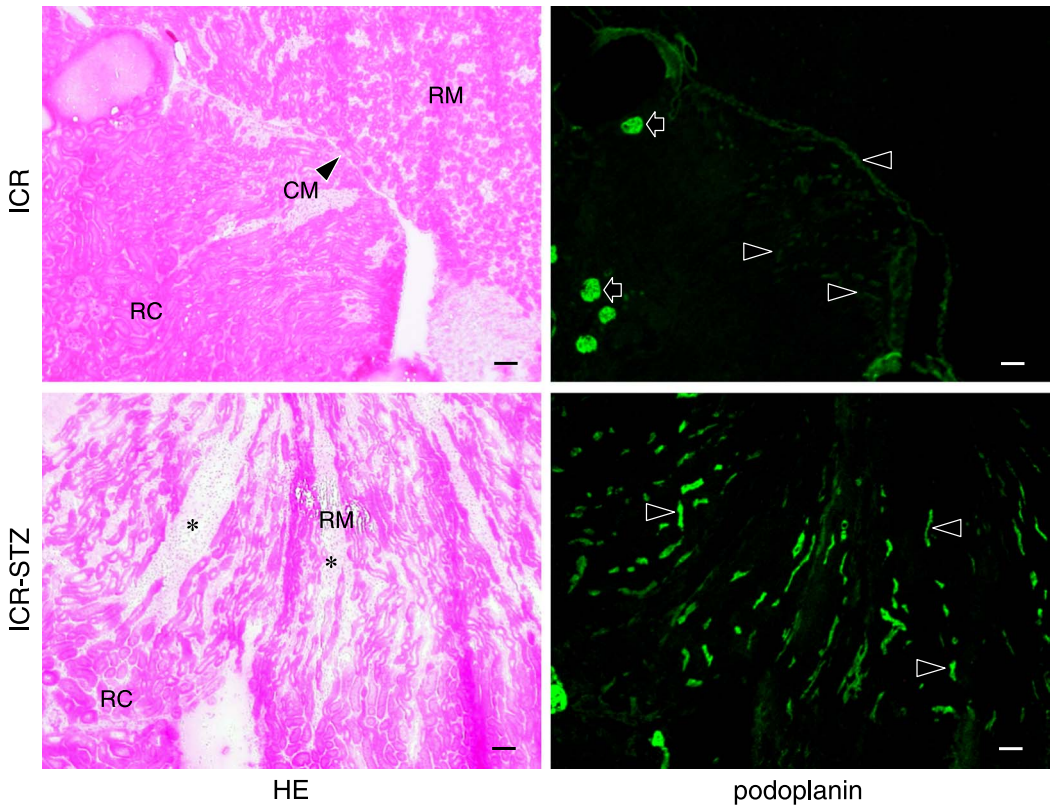

Fig. 3. Distribution of lymphatic vessels in the ICR and ICR-STZ mouse kidneys. The immunostained sections were re-stained by HE staining. The HE staining shows that the kidney tissue is collapsed by edema (asterisks): renal tubules and the peritubular space expanded in the renal medulla (RM) in the ICR-STZ mice compared with the ICR control mice. In the ICR control mice, podoplanin-stained glomeruli (arrows) are present in the renal cortex (RC) near the renal surface and podoplanin-stained lymphatic vessels (arrowheads) are present in the cortex near the cortico-medullary border (CM), but absent in the renal medulla (RM). In the ICR-STZ mice, many podoplanin-stained lymphatic vessels (arrowheads) are present in the cortex and medulla at the expanded peritubular space (asterisks). Bar=100 μm.

double immunostaining. In the ICR, ICR-STZ, KK/Ta, and KK/Ta-HF mouse kidney cortex, anti-podoplanin reacted with glomeruli and lymphatic vessels, while anti-PECAM-1 reacted with blood vessels (Fig. 2). In the low power fields of the ICR control mouse sections, podoplanin-stained glomeruli were present in the cortex near the renal surface and podoplanin-stained lymphatic vessels were present in the cortex near the cortico-medullary border, but absent in the renal medulla (Fig. 3). In the ICR-STZ mice, there were many anti-podoplanin-stained lymphatic vessels in the cortex and medulla at the peritubular space (Fig. 3). There was no hyperplasia or denaturation with cloudy swelling in the tubular epithelial cells, however, it was observed that renal tubules and the peritubular space was expanded in the renal medulla in the ICR-STZ mice. In the low power fields of the KK/Ta control mouse sections, podoplanin-stained glomeruli were present in the cortex near the renal surface and podoplanin-stained lymphatic vessels were present in the cortex near the cortico-medullary border, but absent in the medulla as well as it was absent in the ICR mice (Fig. 4). In the KK/Ta-HF mice, there were many anti-podoplanin-stained lymphatic vessels in the cortex and medulla at the peritubular space and this was also observed in the ICR-STZ mice (Fig. 4). It was further observed that renal tubules and the peritubular space expanded in the renal medulla in KK/Ta-HF mice.

Quantitative analysis for the number of lymphatic vessels in the diabetic mouse kidneys

There were no statistically significant differences in the total numbers of renal blood vessels of the ICR-STZ and ICR control mice, or between the KK/Ta-HF and KK/Ta control mice (Fig. 5). For the number of lymphatic vessels in the kidney tissue, the total numbers and the number of vessels with diameters of 50–100 μm were statistically significant larger in the ICR-STZ mice than in the ICR control mice. There were no statistically significant differences in the numbers of renal lymphatic vessels with diameters below 50 μm or over 100 μm between the ICR-STZ and ICR control mice. The total numbers of lymphatic vessels and the number of vessels with diameters below 50 μm in the kidney tissue were statistically significant larger in the KK/Ta-HF mice than in the KK/Ta control mice. There were no statistically significant differences in the

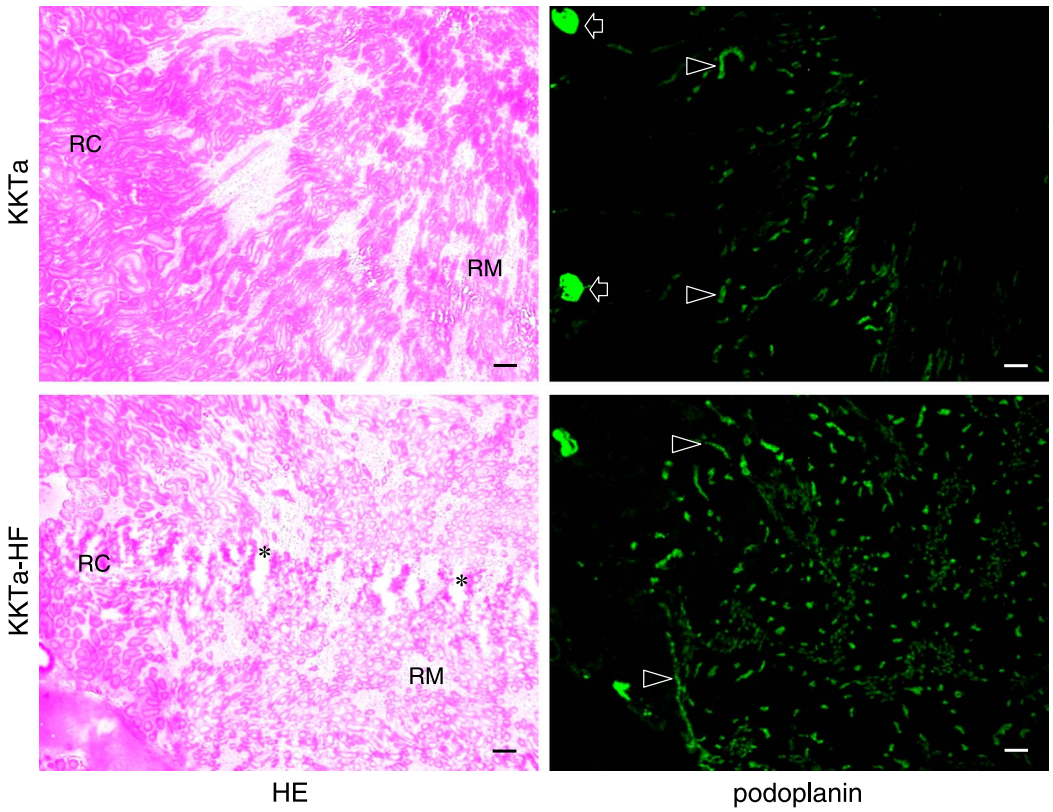

Fig. 4. Distribution of lymphatic vessels in the KKTa and KK/Ta-HF mouse kidneys. The immunostained sections were re-stained by HE staining. The HE staining shows that the kidney tissue is collapsed by edema (asterisks): renal tubules and the peritubular space expanded in the renal medulla (RM) in the KK/Ta-HF mice when compared with the KKTa control mice. In the KKTa control mice, podoplanin-stained glomeruli (arrow) are present in the renal cortex (RC) near the renal surface and podoplanin-stained lymphatic vessels (arrowheads) are present in the cortex near the cortico-medullary border, but absent in the renal medulla (RM). In the KK/Ta-HF mice, many podoplanin-stained lymphatic vessels (arrowheads) are present in the cortex and medulla at the expanded peritubular space (asterisks). Bar=100 μm.

numbers of renal lymphatic vessels with diameters of 50–100 μm or over 100 μm between KK/Ta-HF and KK/Ta control mice.

Quantitative analysis for the area of lymphatic vessels in the diabetic mouse kidneys

There were no significant differences in the anti-PECAM-1-stained renal blood vessel areas of the ICR and ICR-STZ, and between the KK/Ta and KK/Ta-HF mice (Fig. 6). The anti-podoplanin-stained renal lymphatic vessel areas were statistically significant larger in the ICR-STZ than in the ICR, and larger in the KK/Ta-HF than in the KK/Ta mice.

IV. Discussion

The diabetic mouse kidneys showed macroscopic findings of swelling and pale discoloration, and showed histological findings where renal tubules and the peritubular space expanded in the renal medulla of the ICR-STZ mice although there were no hyperplasia and denaturation with cloudy swelling in the tubular epithelial cells. These results suggest that the renal tissue suffered from nephropathy with edema (Fig. 1). The PECAM-1 is commonly expressed on vascular endothelial cells and podoplanin is the marker of lymphatic endothelial cells and podocytes [11, 20]. Further, the expression of podoplanin has been reported on tooth germ epithelial cells and salivary gland myoepithelial cells in somatic tissue [1, 7, 10]. In the mouse heart and kidney tissue, it was confirmed that anti-PECAM-1 reacted with blood vessels, and anti-podoplanin with lymphatic vessels and podocytes (Figs. 1, 2). These results suggest that the immunostaining with the antibodies took place successfully. In both the ICR and KK/Ta control mice, the distribution of lymphatic vessels was observed in the cortex near the cortico-medullary border but not in the cortex near the renal surface, or in the renal medulla (Figs. 3, 4). In both the ICR-STZ and KK/Ta-HF mice, there were many lymphatic vessels with small lumens both in the cortex near the cortico-medullary border and in the medulla at the expanded peritubular space (Figs. 3, 4). It has been established that renal lymphatic vessels are present around large- and middle-sized arteries in the cortex but rarely at the peritubular space in non-diabetic medullas [5, 13,

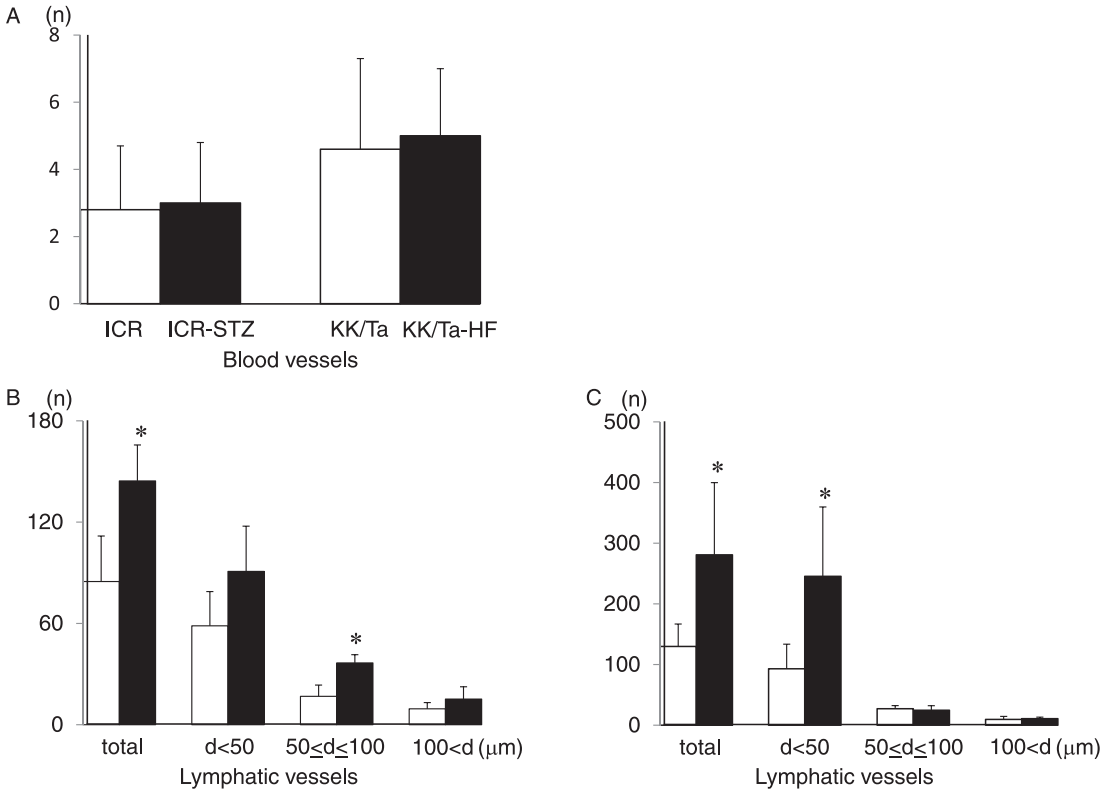

Fig. 5. Quantitative analysis for the numbers of blood and lymphatic vessels in the diabetic mouse kidneys. (**A**) Number of PECAM-1-stained blood vessels in the ICR-STZ and KK/Ta-HF mouse kidneys. There were no statistically significant differences in the total numbers of renal blood vessels between the ICR control and ICR-STZ mice, or between the KK/Ta control and KK/Ta-HF mice. Data are expressed as means±SD. (**B**) Number of podoplanin-stained lymphatic vessels in the ICR-STZ mouse kidneys. There were statistically significant differences in the total numbers of renal lymphatic vessels and in the numbers with diameters (d) of 50–100 μm between the ICR-STZ and ICR control mice. There were no statistically significant differences in the numbers of renal lymphatic vessels with diameters under 50 μm or over 100 μm between the ICR-STZ and ICR control mice. Data are expressed as means±SD. *Significantly different (p<0.01). (**C**) Number of podoplanin-stained lymphatic vessels in the KK/Ta-HF mouse kidneys. There were statistically significant differences in the total numbers of renal lymphatic vessels and in the numbers with diameters (d) under 50 μm between the KK/Ta-HF and KK/Ta control mice. There were no statistically significant differences in the numbers of renal lymphatic vessels with diameters of 50–100 μm or over 100 μm between the KK/Ta-HF and KK/Ta control mice. Data are expressed as means±SD. *Significantly different (p<0.01).

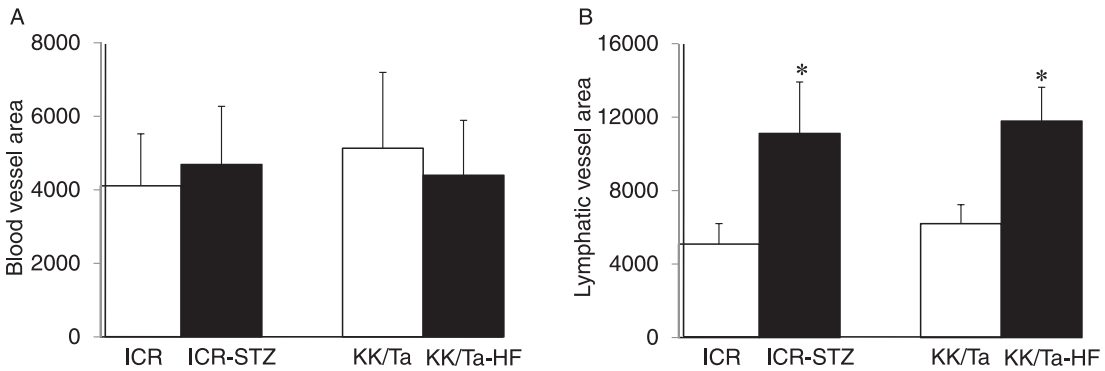

Fig. 6. Quantitative analysis for the area of blood and lymphatic vessels in the diabetic mouse kidneys. (**A**) Area of PECAM-1-stained blood vessels. There were no significant differences in the area of blood vessels in the kidney sections of the ICR and ICR-STZ mice, or between the KK/Ta and KK/Ta-HF mice. (**B**) Area of podoplanin-stained lymphatic vessels. The areas of lymphatic vessels in the kidney sections were statistically significantly larger in the ICR-STZ mice than in the ICR control mice, and larger in the KK/Ta-HF mice than in the KK/Ta control mice. Data are expressed as means±SD. *Significantly different (p<0.01).

18]. Therefore, the results here would suggest that the renal lymphatic circulation increases in diabetic mice with nephropathy.

The total numbers and areas of blood vessels in the renal tissue of the ICR-STZ or KK/Ta-HF mice were similar to those in the ICR or KK/Ta control mice (Figs. 5, 6). Although a progressive glomerulosclerosis finally causes the occlusion of the glomerular capillaries in a diabetic milieu, there may be no significant alteration in the renal microcirculation outside the glomeruli with diabetic nephropathy. Here it is noteworthy that the total numbers and areas of the lymphatic vessels in the renal tissue were statistically significant larger in the ICR-STZ and KK/Ta-HF mice than in the ICR and KK/Ta control mice (Figs. 5, 6). There were also statistically significant differences in the numbers of small lymphatic vessels with diameters of 50–100 μm between the ICR-STZ and the control ICR mice, and in the numbers of lymphatic capillaries with diameters below 50 μm between the KK/Ta-HF and the control KK/Ta mice. Since there were no statistically significant differences in the numbers of renal lymphatic vessels with diameters above 100 μm between the ICR-STZ or KK/Ta-HF diabetic mice and the controls, it is thought that renal lymphangiectasia or the development of initial lymphatics had occurred in the diabetic mouse kidneys with edema. It has been reported that high glucose levels increase the production of TGF-β in proximal tubular cells, glomerular epithelial cells, and mesangial cells, and high glucose and TGF-β coordinately augment the production of excess amounts of vascular endothelial growth factors in renal cells with diabetic conditions [3, 4, 9, 12]. Further, it has been reported that lymphangiogenesis occurs in chronic interstitial nephritis, IgA nephropathy, and myelomatic kidneys [8, 14]. The condition of diabetic nephropathy may allow renal cells to trigger the cytokine network to induce lymphangiogenesis or result in at least the renal lymphatic vessel expansion. Further studies for the cytokine production are required for the renal tissue with diabetic nephropathy.

V. Acknowledgments

This work was supported by Scientific Research (B) 22390345 and Exploratory Research 23659884 grants from Japan Society for the Promotion of Science.

VI. References

1. Amano, I., Imaizumi, Y., Kaji, C., Kojima, H. and Sawa, Y. (2011) Expression of podoplanin and classical cadherins in salivary gland epithelial cells of klotho-deficient mice. *Acta Histochem. Cytochem.* 44; 267–276.
2. Antonetti, D. A., Klein, R. and Gardner, T. W. (2012) Mechanisms of disease: Diabetic retinopathy. *N. Engl. J. Med.* 366; 1227–1239.
3. Chen, S., Hong, S. W., Iglesias-de la Cruz, M. C., Isono, M., Casaretto, A. and Ziyadeh, F. N. (2001) The key role of the transforming growth factor-beta system in the pathogenesis of diabetic nephropathy. *Ren. Fail.* 23; 471–481.
4. Cooper, M. E., Vranes, D., Youssef, S., Stacker, S. A., Cox, A. J., Rizkalla, B., Casley, D. J., Bach, L. A., Kelly, D. J. and Gilbert, R. E. (1999) Increased renal expression of vascular endothelial growth factor (VEGF) and its receptor VEGFR-2 in experimental diabetes. *Diabetes* 48; 2229–2239.
5. Cuttino, J. T. Jr., Clark, R. L. and Jennette, J. C. (1989) Microradiographic demonstration of human intrarenal microlymphatic pathways. *Urol. Radiol.* 11; 83–87.
6. Haneda, M., Koya, D., Isono, M. and Kikkawa, R. (2003) Overview of glucose signaling in mesangial cells in diabetic nephropathy. *J. Am. Soc. Nephrol.* 14; 1374–1382.
7. Hata, M., Amano, I., Tsuruga, E., Kojima, H. and Sawa, Y. (2010) Immunoelectron microscopic study of podoplanin localization in mouse salivary gland myoepithelium. *Acta Histochem. Cytochem.* 43; 77–82.
8. Heller, F., Lindenmeyer, M. T., Cohen, C. D., Brandt, U., Draganovici, D., Fischereder, M., Kretzler, M., Anders, H. J., Sitter, T., Mosberger, I., Kerjaschki, D., Regele, H., Schlondorff, D. and Segerer, S. (2007) The contribution of B cells to renal interstitial inflammation. *Am. J. Pathol.* 170; 457–468.
9. Iglesias-de la Cruz, M. C., Ziyadeh, F. N., Isono, M., Kouahou, M., Han, D. C., Kalluri, R., Mundel, P. and Chen, S. (2002) Effects of high glucose and TGF-beta1 on the expression of collagen IV and vascular endothelial growth factor in mouse podocytes. *Kidney Int.* 62; 901–913.
10. Imaizumi, Y., Amano, I., Tsuruga, E., Kojima, H. and Sawa, Y. (2010) Immunohistochemical examination for the distribution of podoplanin-expressing cells in developing mouse molar tooth germs. *Acta Histochem. Cytochem.* 43; 115–121.
11. Kaji, C., Tsujimoto, Y., Kaneko, M. K., Kato, Y. and Sawa, Y. (2012) Immunohistochemical examination of novel rat monoclonal antibodies against mouse and human podoplanin. *Acta Histochem. Cytochem.* 45; 227–237.
12. Kanwar, Y. S., Wada, J., Sun, L., Xie, P., Wallner, E. I., Chen, S., Chugh, S. and Danesh, F. R. (2008) Diabetic nephropathy: mechanisms of renal disease progression. *Exp. Biol. Med.* 233; 4–11.
13. Kerjaschki, D., Regele, H. M., Moosberger, I., Nagy-Bojarski, K., Watschinger, B., Soleiman, A., Birner, P., Krieger, S., Hovorka, A., Silberhumer, G., Laakkonen, P., Petrova, T., Langer, B. and Raab, I. (2004) Lymphatic neoangiogenesis in human kidney transplants is associated with immunologically active lymphocytic infiltrates. *J. Am. Soc. Nephrol.* 15; 603–612.
14. Kerjaschki, D., Huttary, N., Raab, I., Regele, H., Bojarski-Nagy, K., Bartel, G., Krober, S. M., Greinix, H., Rosenmaier, A., Karlhofer, F., Wick, N. and Mazal, P. R. (2006) Lymphatic endothelial progenitor cells contribute to de novo lymphangiogenesis in human renal transplants. *Nat. Med.* 12; 230–234.
15. Kiguchi, S., Imamura, T., Ichikawa, K. and Kojima, M. (2004) Oxcarbazepine antinociception in animals with inflammatory pain or painful diabetic neuropathy. *Clin. Exp. Pharmacol. Physiol.* 31; 57–64.
16. Mason, R. M. and Wahab, N. A. (2003) Extracellular matrix metabolism in diabetic nephropathy. *J. Am. Soc. Nephrol.* 14; 1358–1373.
17. Mauer, S. M., Steffes, M. W., Ellis, E. N., Sutherland, D. E., Brown, D. M. and Goetz, F. C. (1984) Structural functional relationships in diabetic nephropathy. *J. Clin. Invest.* 74; 1143–1155.
18. McIntosh, G. H. and Morris, B. (1971) The lymphatics of the kidney and the formation of renal lymph. *J. Physiol.* 214; 365–376.
19. Melendez-Ramirez, L. Y., Richards, R. J. and Cefalu, W. T. (2010) Complications of type 1 diabetes. *Endocrinol. Metab. Clin. North. Am.* 39; 625–640.
20. Noda, Y., Amano, I., Hata, M., Kojima, H. and Sawa, Y. (2010)

Immunohistochemical examination on the distribution of cells expressed lymphatic endotheial marker podoplanin and LYVE-1 in the mouse tongue tissue. *Acta Histochem. Cytochem.* 43; 61–68.
21. Phichitrasilp, T., Hondo, E., Rerkamnuaychoke, W., Wakitani, S., Sugiyama, M., Terakawa, J. and Kiso, Y. (2009) Reproductive performance in diabetes mice with a special reference to uterine natural killer cells and placental growth factor. *J. Vet. Med. Sci.* 71; 519–523.
22. Steffes, M. W., Osterby, R., Chavers, B. and Mauer, S. M. (1987) Mesangial expansion as a central mechanism for loss of kidney function in diabetic patients. *Diabetes* 38; 1077–1081.
23. Viljoen, A. and Sinclair, A. J. (2011) Diabetes and insulin resistance in older people. *Med. Clin. North Am.* 95; 615–629.